High-performance aqueous electrolyte symmetrical supercapacitor using porous carbon derived cassava peel waste

by Rika Taslim

Submission date: 28-Apr-2023 01:40PM (UTC+0700)
Submission ID: 2078020415
File name: E,Taer,_23_Ubi_kayu.pdf (2.56M)
Word count: 6434
Character count: 35462

APPLIED
MATERIALS
AND TECHNOLOGY

Research Article

Jamt.ejournal.unri.ac.id

High-performance aqueous electrolyte symmetrical supercapacitor using porous carbon derived cassava peel waste

Erman Taer[1,*], Eva Wahyuni Harahap[1], Apriwandi Apriwandi[1], Rika Taslim[2]

[1]Department of physics, Faculty of Mathematics and Natural Sciences, University of Riau, Simpang Baru, 28293 Indonesia
[2]Department of Industrial Engineering, Faculty of Sciences Technology, Islamic State University of Sultan Syarif Kasim Riau, 28293 Indonesia

ABSTRACT: Electrolytes have generally recognized as one of the most important components in enhancing the electrochemical performance of supercapacitors. On the other hand, aqueous electrolytes considered prime candidates for the development of the next generation of symmetric supercapacitors due to their low-cost, environmentally friendly, high ionic conductivity, fine ionic size, and high capacitance. Herein, the symmetrical supercapacitor of the sustainable porous carbon-based electrode material was confirmed through various aqueous electrolytes consisting of neutral, basic, and acidic such as Na_2SO_4, KOH, and H_2SO_4. Activated carbon obtained from high potential biomass sources of cassava peel waste. Activated carbon synthesis was performed with a comprehensive approach in order to obtain abundant pore structure, high porosity, and improved wettability through a combination of high-temperature chemical and physical activation. In addition, the electrode material is designed to resemble a solid disc without the addition of a synthetic binder. The evaluation of the disc dimensions showed high porosity in the obtained activated carbon. Furthermore, the symmetrical supercapacitor of the optimized electrode material exhibited excellent specific capacitances of 112, 150, and 183 F g^{-1} at 1 mV s^{-1} in the electrolytes Na_2SO_4, KOH, and H_2SO_4, respectively. In addition, the highest rate capability of 70% was confirmed in the H_2SO_4 acid electrolyte. Moreover, their coulombic efficiency can be maintained around 89% with low equivalent series resistance 0.21-0.42 Ω. Therefore, the activated carbon-based supercapacitor symmetric cell device from cassava peel showed high performance for developing high-performance supercapacitor applications with guaranteed stability in aqueous electrolytes.

Key words: aqueous electrolyte; biomass waste; activated carbon; electrode materials; symmetrical supercapacitor

1. INTRODUCTION

The gradual erosion of the atmosphere as a result of the burning of conventional energy resources and the diminishing supply of fossil fuels has diverted the attention of scientists and researchers to explore renewable, sustainable and pollution-free energy [1]. Furthermore, green, effective and efficient technology related to this is highly considered as a critical issue to obtain sustainable energy conversion systems and environmentally friendly energy storage devices. In the last decade, generation III & IV solar cells and fuel cells have been widely pursued by researchers as an effective green energy conversion system that converts solar light energy and chemical energy into stable electricity [2,3]. Meanwhile, researchers are also intensively developing energy storage devices in two main forms of electrochemical devices, namely batteries and supercapacitors, which represent the extraordinary performance of energy storage systems [4,5]. However, cost management mechanisms and harmful by-products are the main focus on the advantages and disadvantages of these devices. From the point of view of electrochemical performance effectiveness, supercapacitors have significant advantages at large power density, increased energy density, countless life cycles, and flexible stable chamber operating temperatures, enabling their application in electrical machinery, electronic components market, and dynamic energy systems [6,7]. However, increasing the energy density of supercapacitors is very important to note to expand their application to a wider range of technologies to support the energy evolution of the modern world.

The main component that needs to be modified to produce high energy density in supercapacitor devices is the basic electrode material. Recent studies reported that the ideal electrode should have high surface area, hierarchical pore distribution, wettability, large electrolyte conductivity, good thermal and chemical stability, and high corrosion resistance which contribute greatly to enhanced specific capacitance, increased energy density, without sacrificing power density of the supercapacitor device [8,9]. Metal oxide materials and conduction polymers as electrode materrials have surprisingly excellent physical properties at high electrical conductivity and confirmed flexibility that can increase the energy density of supercapacitors up to 10 times greater than in previous studies [10,11]. Furthermore, through the template method, they were able to regulate the 3D hierarchical connected pore size distribution enhancing

Received : February 08, 2023
Revised : March 15, 2023
Accepted : March 17, 2023

the electrochemical high performance of the supercapacitor. This is certainly a separate consideration in optimizing electrochemical work devices [12,13]. However, complicated techniques followed by raw materials that are considered expensive are their negative considerations. In addition, unfriendly, toxic by-products and high corrosive properties hinder the development of sustainable materials. Recently, carbon-based electrode materials have attractive properties for energy storage devices due to their relatively inexpensive synthesis route, inexpensive original material, high conductivity, tunenable nanostructure, excellent thermal and chemical stability [14,15]. Moreover, the biomass-based porous carbon in the EDLC type supercapacitor system which presents the breakthrough performance, due to the large surface area, wettability of the self-doping, unique morphological structure which markedly increases the capacitance and energy density is remarkable. In addition, their abundant, sustainable, non-corrosive properties and zero residual discharge allow porous carbon to be a prime candidate as an electrode material for green and sustainable supercapacitors [16,17]. However, they have their own drawbacks such as low energy density compared to metal oxide/conducting polymer materials. Therefore, a reasonable solution is needed to overcome this problem in order to achieve an environmentally friendly supercapacitor product based on porous carbon from biomass.

Recently, it has been known that electrolyte stability is the most critical parameter in improving the electrochemical performance of porous carbon-based supercapacitors by increasing the operating voltage window, ionic conductivity, and ionic pore size [18]. Furthermore, organic electrolytes and ionic liquids have shown their achievements in the expansion of the active window of larger voltages up to 3.7V, and they have shown great cyclical stability in capacitor electrochemical devices [19]. However, its low ionic conductivity increased flammability; instability, toxicity, and high price are the main pitfalls limiting its practical prospects. On the other hand, aqueous electrolytes are considered to be less expensive, and toxic-free, and the ion size conforms to the hierarchical pore structure pattern which is very suitable for biomass-based electrode materials. In addition, these features of electrolytes can result in higher energy densities, relatively low series resistance, and high ion diffusion rates in symmetric supercapacitors. Interestingly, aqueous electrolytes display significantly superior conductivity, low cost, environmental friendliness, high mobility, superior protection, and are non-toxic compared to organic and ionic liquid electrolytes [18]. However, it is necessary to study more deeply their potential in the various pores present in biomass-based bovine carbon, plus their relatively lower potential operating window.

Herein, we study the behavior of different aqueous electrolytes (Na_2SO_4, KOH, and H_2SO_4) on porous carbon-based electrode materials for symmetric supercapacitor applications. Porous carbon was prepared from cassava peel waste which was synthesized through chemical impregnation and physical activation approaches. The optimization of the pore morphology structure was evaluated through differences in the concentration of the activating agent solution. Furthermore, the electrode material is designed to resemble a binder-free solid disc. Surprisingly, aqueous electrolytes based on strong acid H_2SO_4 revealed their high potential to enhance the capacitive properties of cassava peel-based carbon electrodes. The specific capacitance obtained from the optimized electrode material in Na_2SO_4, KOH, and H_2SO_4 electrolytes were 112, 150, and 183 F g^{-1}, respectively. Therefore, the 1M H_2SO_4 electrolyte is highly proportional to the porous carbon-based electrode material of cassava peel for a high-performance symmetrical supercapacitor.

2. MATERIALS AND METHOD

2.1 Preparation of electrode material derived biomass-based activated carbon

The activated carbon used in this study was derived from cassava peel waste. The route of cassava peel waste conversion into activated carbon is carried out through a simple, hassle-free, and time-saving technique. The based material is cleaned with distilled water until all the adhering soil is completely removed. After that, the precursors were finely chopped with sizes varying from 1 cm^2 to 3 cm^2. Precursors were dried using a drying oven at 100°C for 36 hours, it should be noted, that changes in mass were recorded every 12 hours to ensure the moisture content was reduced drastically.

Furthermore, the dry precursor was pre-carbonated in an oven in an airtight container at a graded temperature of 50-250°C. After that, the sample was crushed, grounded, and sieved to obtain a homogeneous powder precursor. Chemical activation was focused on the impregnation of $ZnCl_2$ at different amounts of 0.3 mol/L and 0.7 mol/L in 50 gr precursor powder. The chemically activated samples were designed in the form of solid discs by pressing them with a hydraulic press, and the metric ton pressure was set to ±8 tons. Furthermore, the disc solid sample was pyrolyzed (carbonization-physical activation) in one step initiated by carbonization from a temperature of 27°C to 601°C in inert gas and directly followed by physical activation in CO_2 gas to a temperature of 850°C. Finally, the obtained activated carbon precursors were neutralized with DI Water and labeled CPAC3 and CPAC7, representing the activated carbon from the chemically impregnated cassava peel in 0.3 mol/L and 0.7 mol/L solutions. Generally, the preparation of electrode material derived biomass-based activated carbon is shown in Scheme 1.

2.2 Preparation of symmetrical supercapacitor cell

The supercapacitor cell was prepared in a two-layered coin arrangement consisting of activated carbon electrode material based on cassava peel waste without the addition of a binder such as polyvinyl or others. Activated carbon is set in the form of a 9 mm diameter solid disc at 0.21 mm thickness. The separator used was an organic semipermeable membrane from egg shells. Further, the current collector is prepared from stainless steel with a square acrylic-based cell body.

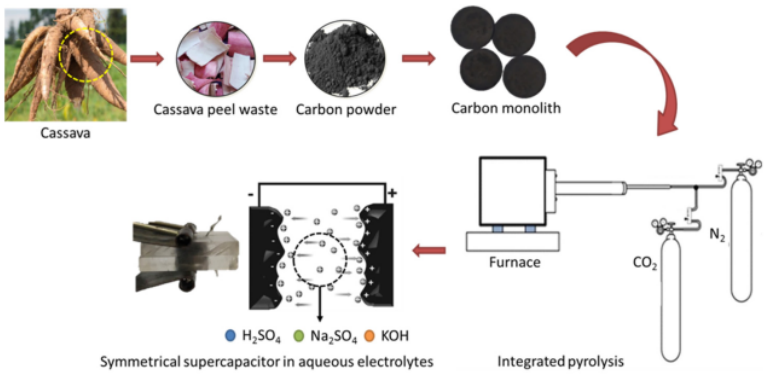

Scheme 1. Preparation of electrode material derived biomass-based activated carbon

2.3. Preparation of aqueous electrolyte solution

Aqueous electrolytes are targeted at three types of electrolyte solutions consisting of neutral/salt, base, and acid supplied from Na_2SO_4, KOH, and H_2SO_4. All three chemicals are dissolved at the same concentration at 1 mol/L. Na_2SO_4 and KOH in the form of pellets/solid were dissolved in a concentration of 1 mol/L in DI water by stirring them on a hotplate stirrer at 300 rpm at 80°C for 60 minutes. Furthermore, a 1 mol/L solution of H_2SO_4 was obtained by diluting 98% H_2SO_4 in 1000 mL DI water.

2.4. Characterization of material properties

The material-porosity properties of cassava peel-based activated carbons designed to resemble discs were evaluated by their dimensional shrinkage in high-temperature pyrolysis. The dimensions of the solid disc including mass, thickness, and diameter were measured before the pyrolysis process. Furthermore, the same thing is also done after the pyrolysis process is complete. The results of the two measurements were compared comprehensively.

2.5. Measurement of electrochemical performance

The performance of electrode materials on various types of aqueous electrolytes is evaluated through comprehensive general methods including cyclic voltammetry (CV), galvanostatic charge-discharge (GCD), and electrochemical impedance spectroscopy (EIS) in a symmetrical supercapacitor system. In detail, the CV technique was reviewed on a potential scale of 0-1V at scan rates of 1, 2, and 5 mV s^{-1}. Furthermore, the GCD method was evaluated in current densities of 1, 2, 5, and 10 A at a scan rate of 1 mV s^{-1}. Moreover, the EIS technique is carried out in the low-frequency range of 100 mHz to 100 kHz high-frequency with an amplitude of 10. Electrochemical parameters such as specific capacitance, electrode/cell/electrolyte resistance, coulombic efficiency, relaxation time constant are calculated through general equations widely reported previously.

3. RESULTS AND DISCUSSION

Biomass waste as a raw material for the synthesis of activated carbon which is designed to resemble a solid disc is certainly easy to experience a decrease in its dimensions in the high-temperature pyrolysis process [20]. It can be easily predicted that the mass of precursors decreases drastically with their diameter and thickness. In detail, the tabulation of the decrease in solid disk dimensions of activated carbon is shown in Fig. 1.

The decrease in mass, thickness, and diameter of the solid disk occur due to the carbonization process, physical activation of CO_2, and chemical reactions of $ZnCl_2$ impregnation [21]. In raw biomass, cassava peels are known to contain large amounts of water and volatiles thus their evaporation at low temperatures tends to decrease disk dimensions in the temperature range of 100-240°C. The removal of the absorbed water content followed by volatile evaporation and the decomposition of hemicellulose that occurs tends to reduce the mass of the disc [22]. The increase in the higher pyrolysis temperature in the inert gas decomposes the cellulose and lignin partially which is characterized at a temperature of >260°C. The concomitant degradation of bio-ligno-cellulose compounds that accompanies the release of H_2O is closely related to a significant decrease in disc mass, diameter, and thickness. At the end of the carbonization process, volatiles, water, hemicellulose, and simple organic components have been removed optimally thus initiating high biochar production [23].

However, their fragile physical condition and suboptimal exploitation of the pore framework are not favorable as electrode materials for energy storage devices. Therefore, it is necessary to treat $ZnCl_2$ chemical reaction and physical activation of CO_2. The chemical reaction of $ZnCl_2$ that occurs at a temperature of 600°C and above allows the etching of carbon chains to initiate the formation of various rich pores [24]. Increasing the concentration of $ZnCl_2$ significantly decreases the mass, thickness, and diameter of the solid disc, as shown in Fig. 1. This proves that chemical impregnation with higher amounts allows the etching of high carbon chains thereby growing new pores, opening narrow pores, and expansion of pores to the meso-macro scale in the precursor. As a consequence, excessive scraping reduces their diameter, thickness, and carbon purity. Furthermore, CO_2 physical activation required to strengthen the resulting pore framework thereby confirming the presence of multiple pores in the activated

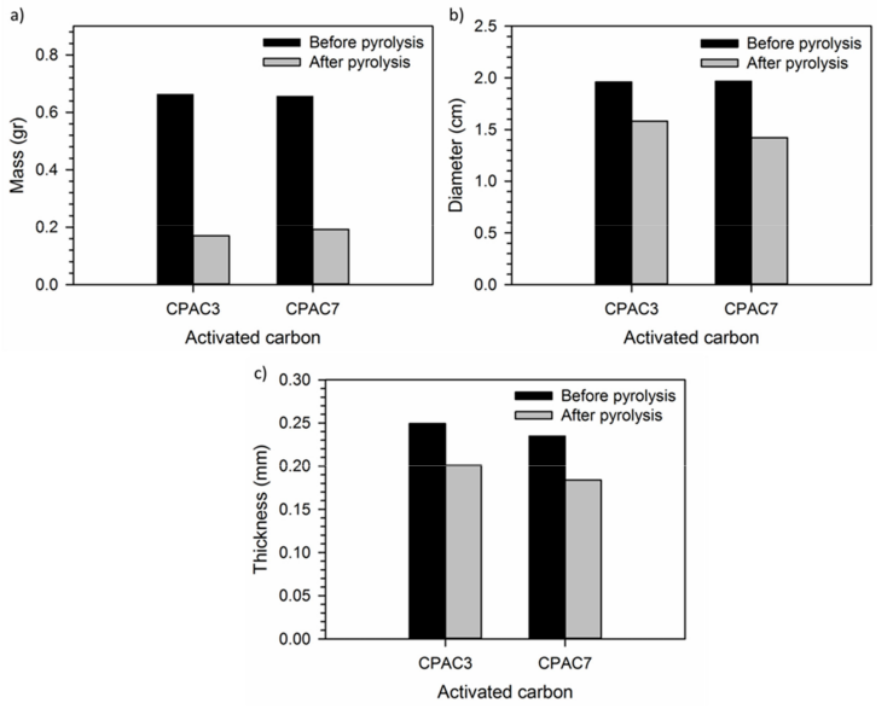

Fig. 1. Reduction of mass, diameter, and thickness in carbonization-physical activation process.

carbon. As reported by various works of literature, the CO_2 activating agent reacts with the carbon content of the precursor via $C + CO_2 \rightarrow 2CO$. As a result, the evaporated carbon monoxide leaves pores on the surface of the precursor. This feature is needed to improve the performance of supercapacitor electrode materials [25]. This analysis was confirmed in depth through electrochemical measurements.

The electrochemical performance of supercapacitors based on CPACs activated carbon electrode materials on different aqueous electrolytes was reviewed comprehensively through a CV approach at a scan rate of 1-5 mV s^{-1}. The CPAC3 and CPAC7 electrodes were evaluated in the neutral, base and acidic electrolytes of Na_2SO_4, KOH, and H_2SO_4 in a symmetrical supercapacitor system, as shown in Fig. 2a and Fig. 2b. In general, the electrodes of CPACs possess a rectangular perturbed CV profile in all aqueous electrolyte solutions. This confirms the development of an electrically rich double layer as a result of aqueous electrolytes having high electrical conductivity compared to organic and ionic liquid electrolytes [26,27]. Electrolytes play an important role in the performance of electrodes to carry out the phenomenon of charge storage. The electrolytes in supercapacitors play an important role in the development of their electrical double layer [28]. Furthermore, the electrolyte also affects the reversible redox reaction of the pseudocapacitive capacitor, as discussed in the previous study [29,30]. It has been widely reviewed that aqueous electrolytes are believed to optimize the formation of abundant electrical double layers in porous carbon-based electrode materials because higher electrical conductivity and low equivalent series resistance initiate better supercapacitor power delivery [18]. In more detail, the ion concentration, cation-anion conductivity, ion size, type, and interaction with the electrode material are important factors in exhibiting capacitive properties and optimizing the performance of activated carbon-based electrode materials, as well as in this study. The significant difference in the hysteresis loops displayed on the CPAC3 and CPAC7 electrodes was significantly influenced by the specifications of the features present in neutral, basic, and acidic electrolytes. The CPAC3 electrode showed a small CV profile with a rectangular shape resembling a matted leaf in a neutral Na_2SO_4 electrolyte solution with a specific capacitance of 112 F g^{-1}.

Furthermore, the basic KOH solution displays a near-ideal and larger rectangular CV profile with an increased specific capacitance of 150 F g^{-1}. Surprisingly, the acid electrolyte H_2SO_4 displayed the largest capacitive property of 183 F g^{-1} with the largest CV profile. In addition, ion degradation is also found in the CV profile, which initiates a faradaic redox reaction in the CPAC3 electrode material. The CV profile of the CPAC7 electrode also displays a similar behavior, where the neutral electrolyte exhibits a weak capacitive property of 118 F g^{-1}. Increasing the alkaline nature of the KOH electrolyte can increase the specific capacitance of the electrode up to 160 F g^{-1}. Furthermore, the highest specific capacitance of the CPAC7 electrode was shown in the H_2SO_4 acid electrolyte of

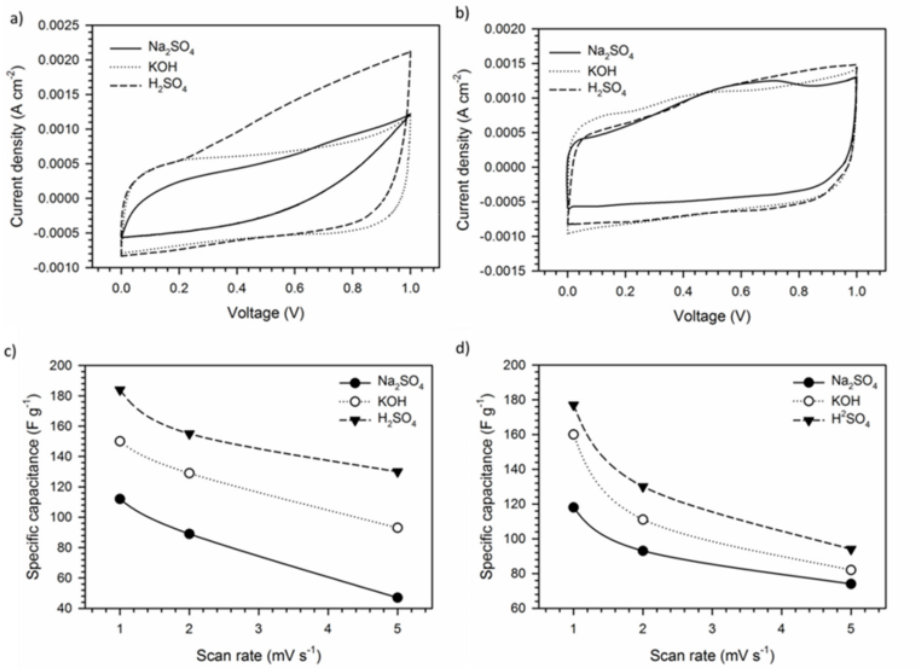

Fig. 2. a) CV curve of CPAC3 in different electrolyte, b) CV curve of CPAC7 in different electrolyte, c) Curve of specific capacitance at different scan rate of CPAC3, and d) Curve of specific capacitance at different scan rate of CPAC7.

176 F g^{-1}. Therefore, the capacitive behavior of the electrochemical capacitors CPAC3 and CPAC7 confirmed the increase in their specific capacitance respectively of electrolyte, neutral, basic, and acidic with the provision of increasing H_2SO_4>KOH>Na_2SO_4. This is due to several factors of the features possessed by each aqueous electrolyte including ionic size, ionic molar conductivity, and the type of interaction that occurs between them. The neutral electrolyte Na_2O_4 has the largest cation and anion radii where the size of the Na^+ ions is 0.95 Å and SO_4^{2-} is 2.30 Å with their low ionic molar conductivity 5.01 and 16.00 ms m^2 mol^{-1}, respectively, showing the lowest capacitive properties for CPAC electrodes [19,31]. Furthermore, the basic electrolyte KOH has smaller ion size specifications of 1.38 Å and 0.46 Å for cation K^+ and anion OH^-, respectively. In addition, their high ionic molar conductivity of 19.91 ms m^2 mol^{-1} and 7.32 ms m^2 mol^{-1} allows the formation of a dense electrical double layer and accessibility of charge on the electrode surface of the CPACs. Moreover, the H_2SO_4 electrolyte has an H^+ cation size that is almost 6 times smaller than K^+, and Na^+ allows these ions to access all active channels on the electrode material. This significantly produces abundant electrochemical coatings [32]. In addition, the outstanding electrical conductivity of H_2SO_4 350 ms m^2 mol^{-1} enables the electrodes of the CPACs to reveal optimum electrode performance with specific capacitances of 183 and 176 F g^{-1} for CPAC3 and CPAC7, respectively. Furthermore, the effect of natural, alkaline and acidic electrolytes was further evaluated at different scanning rates from 1 mVs^{-1} to 5 mVs^{-1}, and it significantly affected the high capacitive properties of the CPACs electrodes, as shown in Fig. 2c and Fig. 2d. The CPAC3 electrode displayed a significant decrease in specific capacitance at scanning rates of 5 mV s^{-1} of 47, 93, and 130 F g^{-1} for aqueous electrolytes of Na_2SO_4, KOH, and H_2SO_4. However, they did show significantly higher capability rates of 41%, 62%, and 70% of Na_2SO_4, KOH, and H_2SO_4 electrolytes. This phenomena shows that the pores that develop in CPAC3 are relatively small and abundant, making it difficult to access the Na_2SO_4 electrolyte which incidentally has a larger bare ion size with a low capability rate of 41% at 5 mV s^{-1}. On the other hand, they are more accessible to the H_2SO_4 electrolyte which has a relatively much smaller bare ion size resulting in a 70% capability rate at 5 mVs^{-1}. On the other hand, the CPAC7 electrode revealed decreased rate capability from neutral to alkaline and to acidic electrolytes by 62%, 51%, and 53% for aqueous electrolytes Na_2SO_4, KOH, and H_2SO_4, respectively. This feature confirms that the CPAC7 electrode has a large pore size with a relatively low active site making it suitable only for neutral electrolytes [33]. On the plus side, these electrodes can be applied over a larger potential window up to 1.8 V, as revealed in a previous study.

Meanwhile, the comparison of the performance of CPAC3 and CPAC7 electrodes in the best electrolyte H_2SO_4 at a scan rate of 1 mV s^{-1} is confirmed in Fig. 3a. Both electrodes exhibit almost normal rectangular hysteresis loops revealing the dominant double-layer electrochemical behavior. Interestingly, the CPAC3 electrode displayed a larger hysteresis loop with a specific capacitance of 183 F g^{-1},

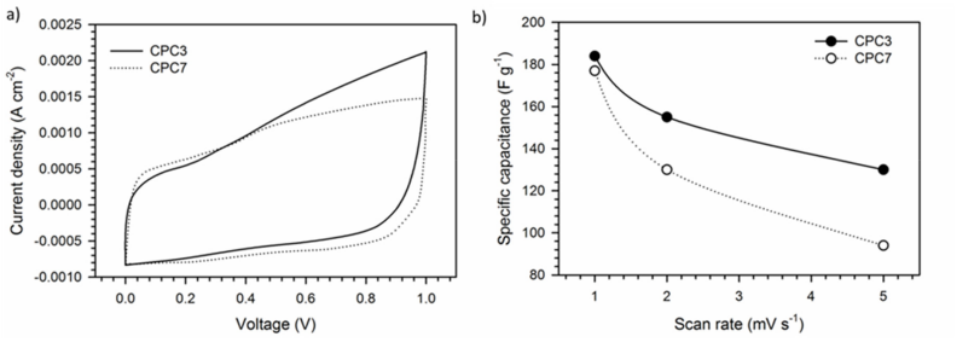

Fig. 3. a) CV curve of CPAC3 and CPAC7 in H_2SO_4 electrolyte at 1 mV s^{-1}, and b) Curve of specific capacitance at different scan rate of CPAC3 and CPAC7 in H_2SO_4 electrolyte.

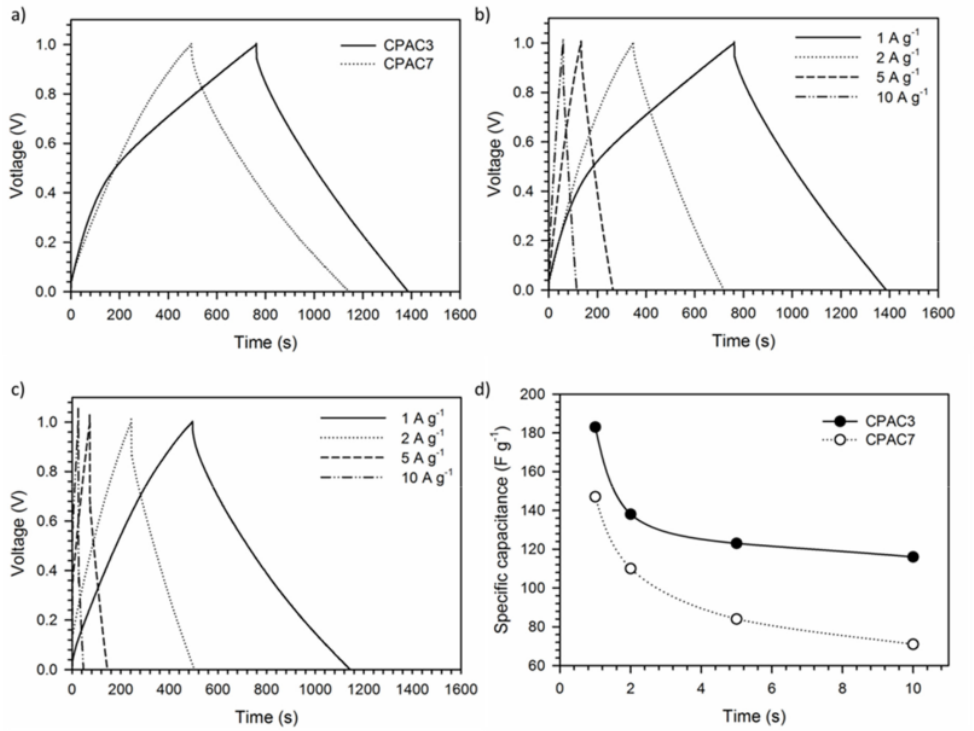

Fig. 4. a) GCD profile of CPACs, b) GCD profile of CPAC3 in different current density, c) GCD profile of CPAC7 in different current density, and d) Curve of specific capacitance at different current density in H_2SO_4 electrolyte.

whereas CPAC7 showed a specific capacitance of 176 F g^{-1}. This event is due to the different porosity properties of the two electrodes. Impregnation of $ZnCl_2$ in 0.3 mol/L solutions allows activated carbon to produce high pore diversity properties thus providing more active channels and shorter charge migration paths [34].

Increasing the concentration of the chemical activating agent solution of 0.7 mol/L allows excessive carbon chain etching which damages the pore structure of the base material and hinders the accessibility of ions. At higher scan rates, their capacitance clearly affects the pore structure that develops on the electrodes of CPACs. In H_2SO_4 electrolyte, CPAC3 can maintain its high specific capacitance with a high capability rate of 70% compared to CPAC7 electrode which only maintains of 53% (see Fig. 3b). This confirms the high performance of the CPAC3 electrode for symmetric supercapacitor applications in the 1M H_2SO_4 electrolyte [35].

The electrochemical performance of the CPAC3 and CPAC7 electrodes in the best aqueous electrolyte of H_2SO_4 was confirmed more thoroughly through GCD measurements, as represented in Fig. 4. Fig. 4a displays the

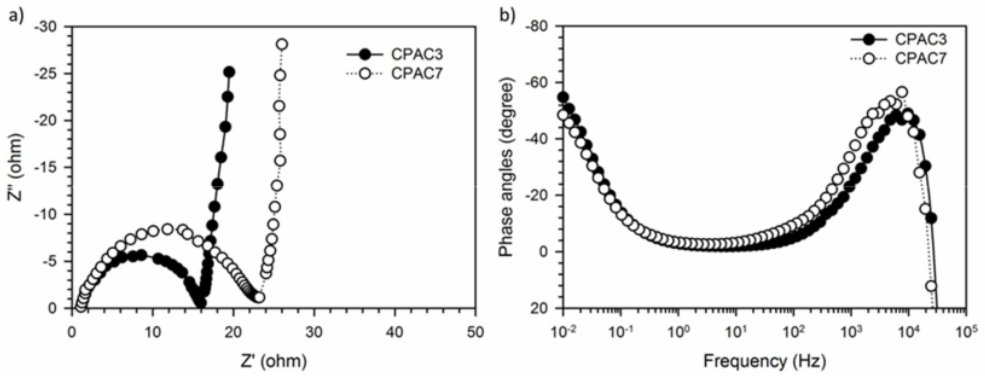

Fig. 5. a) Nyquist plot, and b) Bode phase plot of CPAC3 dan CPAC7 in H_2SO_4 electrolyte.

GCD curves of the CPAC3 and CPAC7 electrodes in a supercapacitor symmetrical system, showing the shape of an isosceles triangle that is perturbed revealing the type of EDLCs normal supercapacitor.

Furthermore, the degradation of electrolyte ions was clearly identified which was identified with a coulomb efficiency of <90%. This is because the presence of functional groups N, O, and S as doping heteroatoms in the cassava peel-based activated carbon base material provides a pseudo-capacitance effect as well as confirmed EDLCs [36,37]. In addition, the weak iR drop in the GCD profile reveals maximum ion accessibility in the pore framework of the electrodes with their relatively low series resistances of 0.12 and 0.083Ω, respectively. This proves that the H_2SO_4 electrolyte can access all available active channels on the activated carbon electrodes of CPACs. Moreover, the long process of charging and discharging the GCD profile reflects the specific capacitance of the CPACs electrodes. Based on the standard equation, the specific capacitance obtained from the CPAC3 and CPAC7 electrodes were 184 and 147 F g^{-1}, respectively. Chemically activated and high-temperature carbonization of CPAC3 electrodes allow the precursor cassava peel to produce rich active channels, diverse pore structures, and enhanced wettability thereby initiating high capacitive behavior [38,39].

However, higher activating agent concentration the CPAC7 electrode allows the destruction of the carbon structure as a result of excessive carbon chain etching. This event reduces the porosity of the carbon material so that it gets low capacitive properties. The high capacitive behavior of CPACs is also reviewed at different current densities as shown in Fig. 4b and Fig. 4c. Both electrodes display a consistent isosceles triangular shape confirming the nature of their normal EDLCs. Furthermore, the increase in higher current density surprisingly improved their coulombic efficiencies by 87% and 89% for CPAC3 and CPAC7, respectively. On the other hand, their specific capacitance is also evaluated at each applied current density, as shown in Fig. 4d. The CPAC3 electrode can maintain a specific capacitance of 116 F g^{-1} at 10 A g^{-1} and the CPAC7 electrode maintains a capacitive property of 71 F g^{-1} at 10 A g^{-1}.

Moreover, the symmetrical cell performance of PCAC3 and PCAC7 electrodes on 1M H_2SO_4 electrolyte was studied in more detail by means of electrochemical impedance spectroscopy in the frequency range of 0.001Hz to 100,000Hz with a constant amplitude of 10. Fig. 5a shows the Nyquist plot of the CPAC3 and CPAC7 symmetric supercapacitor devices obtained in an open circuit potential shows an ideal pattern as an energy storage device for EDLCs [40]. The semicircular profile in the high-frequency region reflects the excellent ionic conductivity of the H_2SO_4 electrolyte with an electrolyte ion resistance of about 0.04-0.09Ω. Furthermore, the x-axis intercept reveals the electrolytic ion charge transfer and migration behavior which characterizes abundant porosity proportions and high electrode wettability properties [41]. Significantly, they showed equivalent series resistance of 0.21–0.42 for CPAC3 and CPAC7 cells, respectively. Furthermore, the characteristic Warburg impedance shown at low frequencies reveals a mechanism of electrochemical behavior dominated by anion–cation insertion at the electrolyte/electrode interface. Moreover, the near-ideal vertical curves displayed at lower frequencies indicate that the CPACs cells have near-ideal supercapacitor behavior of EDLs embellished with pseudocapacitance effects. In addition, Fig. 5b displays a Bode phase plot of the CPAC3 and CPAC7 electrodes in the 1M H_2SO_4 electrolyte. At low frequencies, the CPAC3 electrode displays a phase angle of about -60° and the CPAC7 electrode ranges at -55° indicating the capacitive behavior of the normal electrical double layer embellished with the porous carbon-based pseudo-capacitance effect of the biomass [35,42]. These features clearly prove that the symmetric cell sets of CPAC3 and CPAC7 supercapacitors exhibit high performance for developing applications of high -performance supercapacitors with high stability in aqueous electrolytes of 1M H_2SO_4.

4. CONCLUSIONS

In summary, the porous carbon-based electrode material from cassava peel waste studied in depth on aqueous electrolytes as a symmetric energy storage supercapacitor device. The criteria for selecting aqueous electrolytes are complex, including neutral (Na_2SO_4), basic

(KOH), and acid (H_2SO_4) in a solution of 1 mol/L. The porous carbon was obtained through a safe, inexpensive, pollution-free controlled synthesis route in 0.3 and 0.7 mol/L $ZnCl_2$ chemical impregnation solutions. Through the CV approach, the electrochemical properties of the supercapacitor showed its best performance in the H_2SO_4 electrolyte, followed by KOH and Na_2SO_4. Furthermore, the CPACs electrode material designed in the form of a compact disc revealed a high coulombic efficiency performance of up to 89% at 10 A g^{-1}. Moreover, the supercapacitor cell resistance is relatively low with high conductivity found in the aqueous electrolyte H_2SO_4. Therefore, the 1M H_2SO_4 electrolyte is highly proportional to the porous carbon-based electrode material of cassava peel for a high-performance symmetrical supercapacitor.

AUTHOR INFORMATION

Corresponding Author
*Email: erman.taer@lecturer.unri.ac.id

ORCID
Erman Taer : 0000-0003-4463-8252

ACKNOWLEDGMENTS

The research was founded by in *Direktorat Jenderal Pendidikan Tinggi, Riset dan Teknologi,* Republic of Indonesia in master thesis research-postgraduate program scheme, contract No.: 1657/UN19.5.1.3/PT.01.03/2022.

REFERENCES

[1] V. Rountree, Nevada's experience with the renewable portfolio standard, Energy Policy. 129 (2019) 279–. https://doi.org/10.1016/j.enpol.2019.02.010.
[2] X. Li, B. Wei, Supercapacitors based on nanostructured carbon, Nano Energy. 2 (2013) 159–173. https://doi.org/10.1016/j.nanoen.2012.09.008.
[3] BP Statistical Review of World Energy, 2021.
[4] S. Maddukuri, D. Malka, M.S. Chae, Y. Elias, S. Luski, D. Aurbach, On the challenge of large energy storage by electrochemical devices, Electrochim. Acta. 354 (2020) 136771. https://doi.org/10.1016/j.electacta.2020.136771.
[5] S. Dai, Y. Bai, W. Shen, S. Zhang, H. Hu, J. Fu, X. Wang, C. Hu, M. Liu, Core-shell structured Fe2O3@Fe3C@C nanochains and Ni–Co carbonate hydroxide hybridized microspheres for high-performance battery-type supercapacitor, J. Power Sources. 482 (2021). https://doi.org/10.1016/j.jpowsour.2020.228915.
[6] S. Saini, P. Chand, A. Joshi, Biomass derived carbon for supercapacitor applications: Review, J. Energy Storage. 39 (2021) 102646. https://doi.org/10.1016/j.est.2021.102646.
[7] E. Taer, R. Taslim, Brief Review: Preparation Techniques of Biomass Based Activated Carbon Monolith Electrode for Supercapacitor Application, in: AIP Conf. Proc., 2018: pp. 020004-1-020004–4. https://doi.org/https://doi.org/10.1063/1.5021192.
[8] S. Rawat, R.K. Mishra, T. Bhaskar, Biomass derived functional carbon materials for supercapacitor applications, Chemosphere. 286 (2022) 131961. https://doi.org/10.1016/j.chemosphere.2021.131961.
[9] X. Li, J. Zhang, B. Liu, Z. Su, A critical review on the application and recent developments of post-modified biochar in supercapacitors, J. Clean. Prod. 310 (2021) 127428. https://doi.org/10.1016/j.jclepro.2021.127428.
[10] D. Chu, F. Li, X. Song, H. Ma, L. Tan, H. Pang, X. Wang, D. Guo, B. Xiao, A novel dual-tasking hollow cube NiFe2O4-NiCo-LDH@rGO hierarchical material for high preformance supercapacitor and glucose sensor, J. Colloid Interface Sci. 568 (2020) 120–138. https://doi.org/10.1016/j.jcis.2020.02.012.
[11] Z. Lu, J. Foroughi, C. Wang, H. Long, G.G. Wallace, Superelastic hybrid CNT/graphene fibers for wearable energy storage, Adv. Energy Mater. 8 (2018) 1–10. https://doi.org/10.1002/aenm.201702047.
[12] M. Chen, D. Yu, X. Zheng, X. Dong, Biomass based N-doped hierarchical porous carbon nanosheets for all -solid-state supercapacitors, J. Energy Storage. 21 (2019) 105–112. https://doi.org/10.1016/j.est.2018.11.017.
[13] W. Zhang, R.R. Cheng, H.H. Bi, Y.H. Lu, L.B. Ma, X.J. He, A review of porous carbons produced by template methods for supercapacitor applications, Xinxing Tan Cailiao/New Carbon Mater. 36 (2021) 69–81. https://doi.org/10.1016/S1872-5805(21)60005-7.
[14] S. Majid, A.S.G. Ali, W.Q. Cao, R. Reza, Q. Ge, Biomass-derived porous carbons as supercapacitor electrodes-A review, New Carbon Mater. 36 (2021) 546–572. https://doi.org/10.1016/S1872-5805(21)60038-0.
[15] A.R. Selvaraj, A. Muthusamy, In-ho-Cho, H.J. Kim, K. Senthil, K. Prabakar, Ultrahigh surface area biomass derived 3D hierarchical porous carbon nanosheet electrodes for high energy density supercapacitors, Carbon N. Y. 174 (2021) 463–474. https://doi.org/10.1016/j.carbon.2020.12.052.
[16] G. Gou, F. Huang, M. Jiang, J. Li, Z. Zhou, Hierarchical porous carbon electrode materials for supercapacitor developed from wheat straw cellulosic foam, Renew. Energy. 149 (2020) 208–216. https://doi.org/10.1016/j.renene.2019.11.150.
[17] S. Ghosh, S. Barg, S.M. Jeong, K. Ostrikov, Heteroatom-doped and oxygen-functionalized nanocarbons for high-performance supercapacitors, Adv. Energy Mater. 10 (2020) 1–44. https://doi.org/10.1002/aenm.202001239.
[18] M. Sajjad, M.I. Khan, F. Cheng, W. Lu, A review on selection criteria of aqueous electrolytes performance evaluation for advanced asymmetric supercapacitors, J. Energy Storage. 40 (2021) 102729. https://doi.org/10.1016/j.est.2021.102729.
[19] C. Zhao, W. Zheng, A review for aqueous electrochemical supercapacitors, Front. Energy Res. 3 (2015) 1–11. https://doi.org/10.3389/fenrg.2015.00023.
[20] E. Taer, K. Natalia, A. Apriwandi, R. Taslim, A.

Agustino, R. Farma, The synthesis of activated carbon nano fiber electrode made from acacia leaves (Acacia mangium wild) as supercapacitors, Adv. Nat. Sci. Nanosci. Nanotechnol. 11 (2020) 25007. https://doi.org/10.1088/2043-6254/ab8b60.

[21] E. Taer, A. Apriwandi, D. Rama, Solid coin-like design activated carbon nanospheres derived from shallot peel precursor for boosting supercapacitor performance, J. Mater. Res. Technol. 15 (2021) 1732–1741. https://doi.org/10.1016/j.jmrt.2021.09.025.

[22] I.K. Erabee, A. Ahsan, A.W. Zularisam, S. Idrus, N.N.N. Daud, T. Arunkumar, R. Sathyamurthy, A.E. Al-Rawajfeh, A new activated carbon prepared from sago palm bark through physiochemical activated process with zinc chloride, Eng. J. 21 (2017) 1–14. https://doi.org/10.4186/ej.2017.21.5.1.

[23] J.Y. Chen, L. Sun, I.I. Negulescu, B. Xu, Fabrication and evaluation of regenerated cellulose/nanoparticle fibers from lignocellulosic biomass, Biomass and Bioenergy. 101 (2017) 1–8. https://doi.org/10.1016/j.biombioe.2017.03.024.

[24] M. Vinayagam, R. Suresh Babu, A. Sivasamy, A.L. Ferreira de Barros, Biomass-derived porous activated carbon from Syzygium cumini fruit shells and Chrysopogon zizanioides roots for high-energy density symmetric supercapacitors, Biomass and Bioenergy. 143 (2020) 105838. https://doi.org/10.1016/j.biombioe.2020.105838.

[25] A. Apriwandi, E. Taer, R. Farma, R.N. Setiadi, E. Amiruddin, A facile approach of micro-mesopores structure binder-free coin/monolith solid design activated carbon for electrode supercapacitor, J. Energy Storage. 40 (2021) 102823. https://doi.org/10.1016/j.est.2021.102823.

[26] C. Lämmel, M. Schneider, M. Weiser, A. Michaelis, Investigations of electrochemical double layer capacitor (EDLC) materials - A comparison of test methods, Materwiss. Werksttech. 44 (2013) 641–649. https://doi.org/10.1002/mawe.201300122.

[27] L. Luo, L. Luo, J. Deng, T. Chen, G. Du, M. Fan, W. Zhao, High performance supercapacitor electrodes based on B/N Co-doped biomass porous carbon materials by KOH activation and hydrothermal treatment, Int. J. Hydrogen Energy. 46 (2021) 31927–31937. https://doi.org/10.1016/j.ijhydene.2021.06.211.

[28] P. Vadhva, J. Hu, M.J. Johnson, R. Stocker, M. Braglia, D.J.L. Brett, A.J.E. Rettie, Electrochemical Impedance Spectroscopy for All-Solid-State Batteries: Theory, Methods and Future Outlook, ChemElectroChem. 8 (2021) 1930–1947. https://doi.org/10.1002/celc.202100108.

[29] M. Armand, F. Endres, D.R. MacFarlane, H. Ohno, B. Scrosati, Ionic-liquid materials for the electrochemical challenges of the future, Nat. Mater. 8 (2009) 621–629. https://doi.org/10.1038/nmat2448.

[30] H. Tan, J. Tang, J. Kim, Y.V. Kaneti, Y.M. Kang, Y. Sugahara, Y. Yamauchi, Rational design and construction of nanoporous iron- and nitrogen-doped carbon electrocatalysts for oxygen reduction reaction, J. Mater. Chem. A. 7 (2019) 1380–1393. https://doi.org/10.1039/c8ta08870e.

[31] P. Cheng, T. Li, H. Yu, L. Zhi, Z. Liu, Z. Lei, Biomass-Derived Carbon Fiber Aerogel as a Binder-Free Electrode for High-Rate Supercapacitors, J. Phys. Chem. C. 120 (2016) 2079–2086. https://doi.org/10.1021/acs.jpcc.5b11280.

[32] G. Sathyamoorthi, P. Chiochan, M. Sawangphruk, High-rate aqueous/ionic liquid dual electrolyte supercapacitor using 3D graphene sponge with an ultrahigh pore volume, Electrochim. Acta. 327 (2019) 135014. https://doi.org/10.1016/j.electacta.2019.135014.

[33] A. Gopalakrishnan, S. Badhulika, Sulfonated porous carbon nanosheets derived from oak nutshell based high-performance supercapacitor for powering electronic devices, Renew. Energy. 161 (2020) 173–183. https://doi.org/10.1016/j.renene.2020.06.004.

[34] X. Zhang, B. Liu, X. Yan, X. Zhao, Y. Zhang, Y. Wei, Q. Cao, Design and structure optimization of 3D porous graphitic carbon nanosheets for high-performance supercapacitor, Microporous Mesoporous Mater. 309 (2020) 110580. https://doi.org/10.1016/j.micromeso.2020.110580.

[35] M. Jayachandran, A. Raja, T. Maiyalagan, N. Poongodi, T. Vijayakumar, Effect of various aqueous electrolytes on the electrochemical performance of α-MnO2 nanorods as electrode materials for supercapacitor application, Electrochim. Acta. 366 (2021) 137412. https://doi.org/10.1016/j.electacta.2020.137412.

[36] Q. Abbas, R. Raza, I. Shabbir, A.G. Olabi, Heteroatom doped high porosity carbon nanomaterials as electrodes for energy storage in electrochemical capacitors: A review, J. Sci. Adv. Mater. Devices. 4 (2019) 341–352. https://doi.org/10.1016/j.jsamd.2019.07.007.

[37] S.S. Gunasekaran, A. Gopalakrishnan, R. Subashchandrabose, S. Badhulika, Single step, direct pyrolysis assisted synthesis of nitrogen-doped porous carbon nanosheets derived from bamboo wood for high energy density asymmetric supercapacitor, J. Energy Storage. 42 (2021) 103048. https://doi.org/10.1016/j.est.2021.103048.

[38] J. wu, M. Xia, X. Zhang, Y. Chen, F. Sun, X. Wang, H. Yang, H. Chen, Hierarchical porous carbon derived from wood tar using crab as the template: Performance on supercapacitor, J. Power Sources. 455 (2020) 227982. https://doi.org/10.1016/j.jpowsour.2020.227982.

[39] A. Gopalakrishnan, S. Badhulika, Effect of self-doped heteroatoms on the performance of biomass-derived carbon for supercapacitor applications, J. Power Sources. 480 (2020) 228830. https://doi.org/10.1016/j.jpowsour.2020.228830.

[40] R. Vicentini, L.M. Da Silva, E.P. Cecilio, T.A. Alves, W.G. Nunes, H. Zanin, How to measure and calculate equivalent series resistance of electric double-layer

capacitors, Molecules. 24 (2019). https://doi.org/10.3390/molecules24081452.

[41] N.H. Basri, M. Deraman, S. Kanwal, I.A. Talib, J.G. Manjunatha, A.A. Aziz, R. Farma, Supercapacitors using binderless composite monolith electrodes from carbon nanotubes and pre-carbonized biomass residues, Biomass and Bioenergy. 59 (2013) 370–379. https://doi.org/10.1016/j.biombioe.2013.08.035.

[42] N. Yadav, Ritu, Promila, S.A. Hashmi, Hierarchical porous carbon derived from eucalyptus-bark as a sustainable electrode for high-performance solid-state supercapacitors, Sustain. Energy Fuels. 4 (2020) 1730–1746. https://doi.org/10.1039/c9se00812h.

High-performance aqueous electrolyte symmetrical supercapacitor using porous carbon derived cassava peel waste

ORIGINALITY REPORT

13%	8%	6%	4%
SIMILARITY INDEX	INTERNET SOURCES	PUBLICATIONS	STUDENT PAPERS

PRIMARY SOURCES

1	www.ece.nus.edu.sg Internet Source	<1%
2	Submitted to University of Glasgow Student Paper	<1%
3	uwspace.uwaterloo.ca Internet Source	<1%
4	libres.uncg.edu Internet Source	<1%
5	Sebastian M. Geier, Thorsten Mahrholz, Peter Wierach, Michael Sinapius. "Morphology- and ion size-induced actuation of carbon nanotube architectures", International Journal of Smart and Nano Materials, 2018 Publication	<1%
6	W. C. Li, C. L. Mak, C. W. Kan, C. Y. Hui. "Enhancing the capacitive performance of a textile-based CNT supercapacitor", RSC Adv., 2014 Publication	<1%

7	Submitted to Yeungnam University Student Paper	<1 %
8	encyclopedia.pub Internet Source	<1 %
9	Submitted to Deakin University Student Paper	<1 %
10	Kwan-Woo Ko, Tae-Yeon Cho, Dong Seok Ham, Minji Kang, Woo Jin Choi, Seong-Keun Cho. "Preparation of highly adhesive urethane-acrylate-based gel-polymer electrolytes and their optimization in flexible electrochromic devices", Journal of Electroanalytical Chemistry, 2022 Publication	<1 %
11	blog.ump.edu.my Internet Source	<1 %
12	Arun V. Baskar, Gurwinder Singh, Ajanya M. Ruban, Jefrin M. Davidraj et al. "Recent Progress in Synthesis and Application of Biomass‐Based Hybrid Electrodes for Rechargeable Batteries", Advanced Functional Materials, 2022 Publication	<1 %
13	Jie Wang, Ran Ran, Jaka Sunarso, Chao Yin, Honggang Zou, Yi Feng, Xiaobao Li, Xu Zheng, Jianfeng Yao. "Nanocellulose-assisted low-	<1 %

temperature synthesis and supercapacitor performance of reduced graphene oxide aerogels", Journal of Power Sources, 2017
Publication

14	Sirayu Chanpee, Nattaya Suksai, Napat Kaewtrakulchai, Sutee Chutipaijit, Masayoshi Fuji, Apiluck Eiad-Ua. "Nanoporous Carbon from Water Hyacinth Via Hydrothermal Carbonization", IOP Conference Series: Materials Science and Engineering, 2020 Publication	<1 %
15	explora.unex.es Internet Source	<1 %
16	Submitted to Bogazici University Student Paper	<1 %
17	Submitted to Coventry University Student Paper	<1 %
18	faculty.swjtu.edu.cn Internet Source	<1 %
19	napier-repository.worktribe.com Internet Source	<1 %
20	pasca-fisika.unri.ac.id Internet Source	<1 %
21	patents.google.com Internet Source	<1 %

22	Zhiming Cui, Weiyong Yuan, Chang Ming Li. "Template-mediated growth of microsphere, microbelt and nanorod α-MoO3 structures and their high pseudo-capacitances", Journal of Materials Chemistry A, 2013 Publication	<1 %
23	lucris.lub.lu.se Internet Source	<1 %
24	open.library.ubc.ca Internet Source	<1 %
25	research.ku.ac.th Internet Source	<1 %
26	Daniel Gray, David Bernell. "Tree-hugging utilities? The politics of phasing out coal and the unusual alliance that passed Oregon's clean energy transition law", Energy Research & Social Science, 2020 Publication	<1 %
27	dias.library.tuc.gr Internet Source	<1 %
28	ejournal.unri.ac.id Internet Source	<1 %
29	journal.ugm.ac.id Internet Source	<1 %
30	researchers.uq.edu.au Internet Source	<1 %

31	Submitted to American University in Cairo Student Paper	<1 %
32	Michael Pycraft Hughes. "The Influence of Stern Layer Conductance on the Dielectrophoretic Behavior of Latex Nanospheres", Journal of Colloid And Interface Science, 20020601 Publication	<1 %
33	Xu, Guiyin, Hui Dou, Xiumei Geng, Jinpeng Han, Lifeng Chen, and Hongli Zhu. "Free standing three-dimensional nitrogen-doped carbon nanowire array for high-performance supercapacitors", Chemical Engineering Journal, 2017. Publication	<1 %
34	academic-accelerator.com Internet Source	<1 %
35	Zhaoxuan Feng, Karin H. Adolfsson, Yanan Xu, Haiqiu Fang, Minna Hakkarainen, Mingbo Wu. "Carbon dot/polymer nanocomposites: From green synthesis to energy, environmental and biomedical applications", Sustainable Materials and Technologies, 2021 Publication	<1 %
36	Submitted to National University of Singapore Student Paper	<1 %
	Submitted to University of Warwick	

37	Student Paper	<1%
38	nmbu.brage.unit.no Internet Source	<1%
39	e-bnr.org Internet Source	<1%
40	Fri Murdiya, M. Rafi Epapras, Dede Irawan, Amir Hamzah, Firdaus, Suwitno. "High Voltage Plasma Convert Coconut Shell Charcoal To Few Layer Wrinkled Graphene (FLwG)", 2022 3rd International Conference on Electrical Engineering and Informatics (ICon EEI), 2022 Publication	<1%
41	www.ivis.org Internet Source	<1%
42	www.jurnal.ugm.ac.id Internet Source	<1%
43	Submitted to University of Dundee Student Paper	<1%
44	Yilkal Dessie, Sisay Tadesse, Rajalakshmanan Eswaramoorthy. "Review on manganese oxide based biocatalyst in microbial fuel cell: Nanocomposite approach", Materials Science for Energy Technologies, 2020 Publication	<1%
	expeditiorepositorio.utadeo.edu.co	

45	Internet Source	<1%
46	personal.article.dyndns.info Internet Source	<1%
47	Gao, G.H.. "Mutual diffusion coefficients of concentrated 1:1 electrolyte from the modified mean spherical approximation", Fluid Phase Equilibria, 20070801 Publication	<1%
48	Luo, Yang, Tianye Yang, Zhifang Li, Bingxin Xiao, and Mingzhe Zhang. "High performance of Mn3O4 cubes for supercapacitor applications", Materials Letters, 2016. Publication	<1%
49	Submitted to Yakın Doğu Üniversitesi Student Paper	<1%
50	apps.who.int Internet Source	<1%
51	cris.technion.ac.il Internet Source	<1%
52	discovery.researcher.life Internet Source	<1%
53	eprints.um.edu.my Internet Source	<1%
54	hull-repository.worktribe.com Internet Source	

		<1%
55	kirj.ee Internet Source	<1%
56	www.africamrs.co.za Internet Source	<1%
57	www.iieta.org Internet Source	<1%
58	www.scilit.net Internet Source	<1%
59	A.W. Stewart, A. Julien, D. Regaldo, P. Schulz, B. Marí Soucase, D.R. Ceratti, P. López-Varo. "Shedding light on electronically doped perovskites", Materials Today Chemistry, 2023 Publication	<1%
60	Tayyaba Najam, Shumaila Ibraheem, Muhammad Altaf Nazir, Asma Shaheen et al. "Partially oxidized cobalt species in nitrogen-doped carbon nanotubes: Enhanced catalytic performance to water-splitting", International Journal of Hydrogen Energy, 2021 Publication	<1%

Exclude quotes	Off	Exclude matches	Off
Exclude bibliography	Off		